Northumbria Research Link

Citation: Thrivikraman Pillai, Jayasankar, Murtugudde, R. and Eldho, T.I. (2019) The Indian Ocean Deep Meridional Overturning Circulation in Three Ocean Reanalysis Products. Geophysical Research Letters, 46 (21). pp. 12146-12155. ISSN 0094-8276

Published by: American Geophysical Union

URL: https://doi.org/10.1029/2019GL084244 <https://doi.org/10.1029/2019GL084244>

This version was downloaded from Northumbria Research Link: http://nrl.northumbria.ac.uk/id/eprint/47029/

Northumbria University has developed Northumbria Research Link (NRL) to enable users to access the University's research output. Copyright © and moral rights for items on NRL are retained by the individual author(s) and/or other copyright owners. Single copies of full items can be reproduced, displayed or performed, and given to third parties in any format or medium for personal research or study, educational, or not-for-profit purposes without prior permission or charge, provided the authors, title and full bibliographic details are given, as well as a hyperlink and/or URL to the original metadata page. The content must not be changed in any way. Full items must not be sold commercially in any format or medium without formal permission of the copyright holder. The full policy is available online: http://nrl.northumbria.ac.uk/policies.html

This document may differ from the final, published version of the research and has been made available online in accordance with publisher policies. To read and/or cite from the published version of the research, please visit the publisher's website (a subscription may be required.)

Northumbria University NEWCASTLE

University Library

Check for updates

AGU100 ADVANCING EARTH AND SPACE SCIENCE

Geophysical Research Letters

RESEARCH LETTER
10.1029/2019GL084244

The Indian Ocean Deep Meridional Overturning Circulation in Three Ocean Reanalysis Products

T. Jayasankar[1], R. Murtugudde[2,1], and T.I. Eldho[1,3]

[1]Interdisciplinary Programme in Climate Studies, Indian Institute of Technology, Bombay, India, [2]ESSIC, University of Maryland, College Park, MD, USA, [3]Department of Civil Engineering, Indian Institute of Technology, Bombay, India

Key Points:
- The inferred IO deep MOC consists of two deep and strong counterclockwise cells located south of 30°S and around 10°S, respectively
- The geostrophic contribution along with the barotropic mode dominates the cell located south of 30°S
- A combination of Ekman and geostrophic components dominates the cell located at 10°S

Supporting Information:
- Supporting Information S1

Correspondence to:
T. I. Eldho,
eldho@civil.iitb.ac.in

Citation:
Jayasankar, T., Murtugudde, R., & Eldho, T. I. (2019). The Indian Ocean deep meridional overturning circulation in three ocean reanalysis products. *Geophysical Research Letters*, *46*, 12,146–12,155. https://doi.org/10.1029/2019GL084244

Received 25 JUN 2019
Accepted 8 OCT 2019
Published online 3 NOV 2019

Abstract The time mean Indian Ocean (IO) deep meridional overturning circulation (MOC) is compared across three ocean reanalysis products (ORAS4, GECCO2, and GFDL). The MOC stream functions obtained by vertically integrating the mass flux across a latitude-depth section in three products are found to be significantly different from each other. Detailed analysis suggests that ORAS4 delivers the best depiction of IO MOC. The inferred IO deep MOC consists of two deep and strong counterclockwise cells located south of 30°S and around 10°S, respectively. The geostrophic component along with the barotropic or external mode dominates the former, and a combination of Ekman and geostrophic components dominates the latter. GECCO2 depicts a steady decline in the northward meridional transport in the bottom layer and a consequent reduction in the MOC strength. The tropical thermocline in GECCO2 responds to this MOC variability leading to rapid and monotonic warming of the tropical IO.

Plain Language Summary Reanalysis products are comprehensive records produced by merging data and models. They are extensively used to study ocean dynamics and thermodynamics of the past. However, depending on model configurations and surface forcings used, these products can differ from one another. We compare three ocean reanalysis products (ORAS4: Ocean Reanalysis System 4, GECCO2: German contribution to the consortium for Estimating the Circulation and Climate of the Ocean 2, and GFDL: Ensemble Coupled Data Assimilation system by Geophysical Fluid Dynamics Laboratory) in the context of the Indian Ocean (IO) deep meridional overturning circulation (MOC). MOC consists of a system of warm poleward surface currents and cold equatorward deep currents as a part of the global poleward oceanic heat transport. ORAS4 delivers the best depiction of Indian Ocean deep MOC. The geostrophic component along with the external mode dominates the circulation south of 30°S, and a combination of Ekman and geostrophic components dominates the circulation at 10°S. The rapidly warming IO has global coupled climate impacts, and a rapidly warming Southern Ocean transmits its signal to the IO via the MOC. Accurate representation of these processes is critical for understanding and monitoring the global heat balance in a warming world.

1. Introduction

The Indian Ocean (IO) meridional overturning circulation (MOC) is an integral component of the global thermocline circulation as well as the regional climate variability and change. Despite its importance, the IO MOC is relatively unexplored compared to other oceans (Balmaseda et al., 2007; Fujii et al., 2017; Karspeck et al., 2017; Murtugudde & Annamalai, 2004; Sime et al., 2006). Lee and Marotzke (1998) studied the IO MOC using a global circulation model based on a monthly averaged climatological forcing. Later, Wang et al. (2012, 2014) studied the deep IO MOC using an ocean reanalysis product, namely, German contribution to the consortium for Estimating the Circulation and Climate of the Ocean 2 (GECCO2). However, there is a difference in the mean annual IO MOC stream function or the MOC structure presented in the two studies. Unlike Lee and Marotzke (1998), Wang et al. (2012) inferred a double core mean MOC stream function (at depths 1,500 and 3,200 m, respectively) that occupy the latitudinal band 30°S to 25°S, and together they account for 2.1 Sv of inflow at deeper ocean depths (deeper than 1,500 m) and exit at intermediate depths (between 700 and 1,500 m). As per their study, the deep circulation cell is strongest south of 25°S and diminishes northward. Wang et al. (2012) also reported a steady decline over the period of study (1961–2000) in the bottom layer transport into the IO at 34°S in GECCO2. Increased data availability and computational resources since Lee and Marotzke (1998) have benefitted not only GECCO2 but the other reanalysis products as well, and thus they can all be contrasted fairly for the processes they represent. A process study with multiple products can offer critical insights into the uncertainties in the IO MOC, especially in the

©2019. American Geophysical Union. All Rights Reserved.

data-poor deep ocean regions. The structure of the IO MOC is thus investigated among three Ocean reanalysis products (Ocean Reanalysis System 4 [ORAS4], GECCO2, and Geophysical Fluid Dynamics Laboratory [GFDL]). The bottom layer meridional transport into the IO is also investigated to contrast the declining trend reported in GECCO2 against other products. We then employ GECCO2 to investigate the tropical upper ocean response to its declining bottom layer transport since surface warming can have direct and fast feedbacks to the coupled climate system

2. Materials and Methods

2.1. Data

The three ocean reanalysis products used are the ORAS4 (Balmaseda et al., 2013), GECCO2 (Köhl, 2015) and Ensemble Coupled Data Assimilation system by GFDL (Zhang et al., 2007). The atmospheric products with which the ocean reanalysis products are forced are also contrasted for computation of Ekman transport. ORAS4 is forced with the European Centre for Medium-Range Weather Forecasts products (Dee et al., 2011; Uppala et al., 2005). GECCO2 and GFDL are forced with National Centers for Environmental Prediction surface fluxes (Kalnay et al., 1996).

2.2. Methodology

Our focus here is mainly on the MOC stream function and its decomposition. The stream function on a latitude-depth plane of the basin is computed by integrating the meridional mass flux at its zonal section from east to west followed by bottom to top up to the depth of interest. Hence, a positive (negative) stream function indicates a counterclockwise (clockwise) circulation with northward (southward) flowing deep layers and southward (northward) flowing upper layers. By bottom to top integration, the influence of Indonesian throughflow (ITF, supporting information Text S1) on the stream function can be avoided as our interest is the deep MOC.

The MOC is decomposed into its components, namely, geostrophic, Ekman, and external mode. The methodology adopted is based on Lee and Marotzke (1998) and Sime et al. (2006). The meridional velocity (υ) at a point on a zonal section is decomposed as the sum of mean sectional velocity ($\overline{\upsilon}$), geostrophic component (υ_ρ), Ekman component (υ_τ), external mode (υ_*), and a residual term (υ_R). The residual term is expected to accommodate errors and ageostrophic components.

$$\upsilon(x,y,z,t) = \overline{\upsilon}(y,t) + \upsilon_\rho(y,z,t) + \upsilon_\tau(x,y,z,t) + \upsilon_*(x,y,t) + \upsilon_R(x,y,z,t) \tag{1}$$

$$\upsilon_\rho = -\frac{1}{\rho_0 f}\left\{\left[g\int_{-h_b}^{0}\frac{\rho_e-\rho_w}{L(Z)}\mathrm{d}Z\right]-\left[\frac{g}{h_b}\int_{-h_b}^{0}\int_{-h_b}^{z}\frac{\rho_e-\rho_w}{L(Z)}\mathrm{d}Z\mathrm{d}z\right]\right\} \tag{2}$$

$$\upsilon_\tau = -\frac{1}{\rho_0 f}\left[\frac{H(z+h_\tau)}{h_\tau}\tau_x-\frac{L(0)\overline{\tau_x}}{A}\right] \tag{3}$$

$$\upsilon_* = (\upsilon_m-\overline{\upsilon})-\frac{1}{\rho_0 f}\left[\frac{\tau_x}{h_b}-\frac{L(0)\overline{\tau_x}}{A}\right] \tag{4}$$

where, x, y, and z are the coordinates in the longitudinal, latitudinal, and vertical (bottom to top) directions, respectively; t is time; ρ is the density; ρ_e and ρ_w are density at the eastern and western boundaries of the basin, respectively; f is the Coriolis parameter and g is the acceleration due to gravity; $L(z)$ is the zonal basin width at a depth z and A is the zonal sectional area; h_b is the local bathymetric depth and h_τ is the Ekman layer depth; τ_x is the zonal winds stress and $\overline{\tau_x}$ is its sectional mean; $H(z)$ is the Heaviside function where its value is 1 when $z >= 0$ and 0 when $z < 0$; and υ_m is the vertical mean velocity. The first set of terms in geostrophic component represents the balance of thermal wind shear and zonal density gradient, and the second set of terms is depth average of the first. The first set of terms in the Ekman component represents the Ekman velocity, and the second set of terms represents the balancing mean sectional return flow. The first set of terms in the external mode represents vertical mean velocity anomaly with respect to sectional mean ($\overline{\upsilon}$), and the second set of terms represents anomalies in the depth-averaged Ekman velocity due to zonal variation of zonal wind stress or bathymetry. Thus, the sectional integrals of all the three components are equal to 0 (details in Text S2). Also, all trends estimated in this study are Theil-Sen (Sen, 1968; Theil, 1950) slopes with 95% significance.

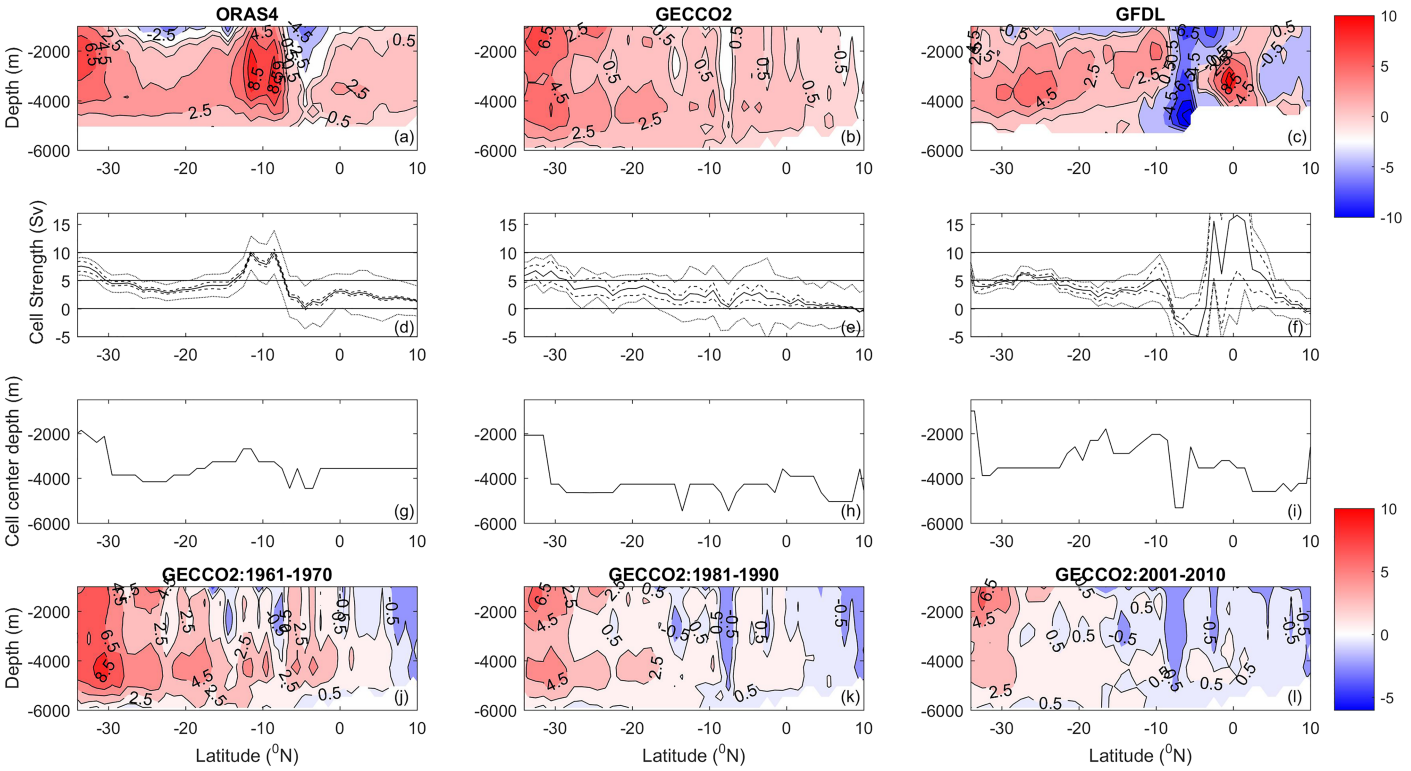

Figure 1. Time mean meridional overturning stream function (sverdrups, positive counterclockwise and negative clockwise) in the Indian Ocean (1961–2010) in (a) ORAS4, (b) GECCO2, and (c) GFDL. The respective maximum counterclockwise cell strength of the deep cells is shown in (d), (e), and (f). The respective depths of maxima are shown in (g), (h), and (i). The thick lines show mean and the dotted/thin lines show the interannual/seasonal standard deviation. Decadal time means of meridional overturning circulation stream function in the Indian Ocean in GECCO2 from 1961 to 2010 (j, k, and l). ORAS4 = Ocean Reanalysis System 4; GECCO2 = German contribution to the consortium for Estimating the Circulation and Climate of the Ocean 2; GFDL = Ensemble Coupled Data Assimilation system by Geophysical Fluid Dynamics Laboratory.

3. IO MOC Stream Function

The time mean structure of IO MOC stream function across the three ocean reanalysis products are presented in this section which offers stark differences (Figures 1a–1i). As the focus is on long-term mean MOC, its standard deviations are shown after filtering out dominant interannual components of periods less than 7 years like the El Niño Southern Oscillation (Pillai & Mohankumar, 2009). The dominant deep MOC cell in ORAS4 is located at 10°S, while in GECCO2 it is located southward of 25°S as presented by Wang et al. (2012). In GFDL the deep cells are not as strong as ORAS4, while to the north of 10°S, the MOC in GFDL gives a strong clockwise circulation in contrast to the other two. However, unlike the time mean structure, all three products agree with each other on seasonal scale, and hence we infer that the differences in them are basically at interannual time scales (Text S3).

To gain further insights, we compare the deep layer transport into the IO. The deep layers are demarcated by the same density classes adopted by Wang et al. (2012) based on Ganachaud and Wunsch (2000) and Ganachaud et al. (2000). They are four layers separated by neutral density surfaces; upper layer ($\gamma^n \leq 27.05$), intermediate layer ($27.05 < \gamma^n \leq 27.72$), deep layer ($27.72 < \gamma^n \leq 28.11$), and bottom layer ($28.11 < \gamma^n$). The depth and thickness of each layer at 34°S in all the three reanalysis products are found to be comparable with each other (Figures S4a–S4c). The time mean meridional flow at 34°S is found to be similar in ORAS4 and GECCO2, while GFDL presents a slightly different picture. As reported by Wang et al. (2012), there is a steady decline in the bottom layer transport at 34°S in GECCO2 (Figure S4d). However, there is no such decline in the other two products; instead there is a steady northward transport at decadal time scales of nearly 7 Sv. The GECCO2 synthesis is available from 1948, and the bottom layer transport in it is found to be declining from the beginning. The magnitude of the bottom layer transport in GECCO2 is similar to the other two in the initial few years (1961–1967) of our analysis, and before 1961, the volume transports

are much larger. The consequent changes in MOC structure due to the decline can be inferred from the time evolution of MOC (Figures 1j–1l). It can be noted that, just as in ORAS4, the positive circulation around 10°S is stronger in GECCO2 in the initial years of analysis and it declines over time to give an MOC structure which is more dominant in the southern IO as shown in Figure 1c which is also seen in Wang et al. (2012).

The slow deep circulation along with the rapid shallow wind-driven circulation are the major components that determine the thermal structure of the ocean (Luyten et al., 1983) which in turn determines the heat budget of the ocean (Boccaletti, Pacanowski, George, Philander, & Fedorov, 2004). The two oceanic circulations together transport heat from low latitudes to high latitudes and balance the ocean heat budget. Consequently, there is a shallow thermocline in the tropics (assisting heat gain) and deep thermocline at high latitudes (driving a heat loss). As per model studies, a reduction in heat loss at the poles or a decline in the circulation would result in anomalous heating of the mixed layer (Boccaletti, Pacanowski, George, Philander, & Fedorov, 2004). This would deepen the equatorial thermocline such that the heat budget remains closed on long time scales. The oceanic diffusivity determines the relative significance of deep and shallow circulations such that low (high) diffusivities favor (disfavor) wind-driven circulation and upwelling (Boccaletti, Pacanowski, George, Philander, & Fedorov, 2004). As the experiments in Boccaletti, Pacanowski, George, Philander, and Fedorov (2004) were carried out for hypothetical ocean basins with climatological easterlies, the equatorial upwelling zones are formed on the eastern boundary forming a cold tongue of shallow thermocline. However, in the IO, there is no cold tongue in the east and the observed upwelling zone is in the west known as the southwest tropical thermocline ridge (Hermes & Reason, 2008). This region is characterized by seasonally changing winds to the north and persistent south easterlies to the south with the resultant Ekman pumping lifting the cool deep waters to form a seasonally varying shallow thermocline (Murtugudde & Busalacchi, 1999). Theories (Text S5) would suggest an upper ocean thermocline response to deep ocean temperature changes (Boccaletti, Pacanowski, George, Philander, & Fedorov, 2004; Boccaletti, Pacanowski, George, & Philander, 2004). Hence, the response of tropical IO to the decline of bottom layer transport in GECCO2 is of great interest especially since the internally generated variability is relatively weaker in the IO than the externally forced variability (Guemas et al., 2013; Ummenhofer et al., 2017). Before we delve into decomposing the MOC into its components, we present the tropical IO response in GECCO2 to the decline in its bottom layer transport into the IO.

4. Tropical IO Response to the Decline in Deep MOC

As per some studies, a decline in MOC is expected to increase the temperature and decrease the heat uptake of the tropical IO and a consequent deepening of the thermocline depth (Boccaletti, 2004; Boccaletti, Pacanowski, George, Philander, & Fedorov, 2004; Boccaletti, Pacanowski, George, & Philander, 2004). The patterns of mean thermocline depth (20°C isotherm) in the IO across all three products are found to be generally similar to each other (Figures 2a–2c) where the thermocline ridge region (Western IO between 15°S and 7°S) is marked by a shallow thermocline. However, as expected, the spatial patterns of trends in thermocline depth in GECCO2 are found to be different from that of the other two (Figures 2d–2f). A cooling in the subsurface layers of tropical IO, especially the thermocline ridge region, and consequent decreasing trend in sea level anomaly as well as thermocline depth in the past few decades are well documented (Han et al., 2010; Schwarzkopf & Böning, 2011). It is inferred to be due to increased upwelling caused by the warming-driven intensification of the local Walker and Hadley cells. Both ORAS4 and GFDL are able to reproduce the same (Figures 2d and 2f) but not GECCO2 (Figure 2e). In GECCO2, the negative trends are observed to be nullified completely in the eastern IO and partially in the western IO. This can be anticipated based on the studies that have pointed out that there is a dominance of wind-induced Ekman pumping in the tropical western IO (west of 80°E) compared to eastern IO which is mainly influenced by the Pacific Ocean via the ITF (Jin et al., 2018; Murtugudde et al., 1998; Valsala et al., 2010; Zhuang et al., 2013).

The latitude-depth sections of temperature trends for the eastern and western IO are presented in Figures 2g–2l. It can be noted that there is a strong cooling trend in the tropical subsurface IO (between 20°S and 10°S and between 50 and 400 m) in both ORAS4 and GFDL. Also there is a strong heating trend in the western tropical subsurface IO (around 40°S) in all three reanalysis products. Similar trends can also be inferred from ocean observations of Levitus et al. (2005), and the cooling trend amidst heating elsewhere has been attributed to shoaling of thermocline due to increasing trend in Ekman pumping (Han et al., 2006). Previous studies have explored the causes of these subsurface temperature trends (Alory et al., 2007; Du & Xie, 2008) and

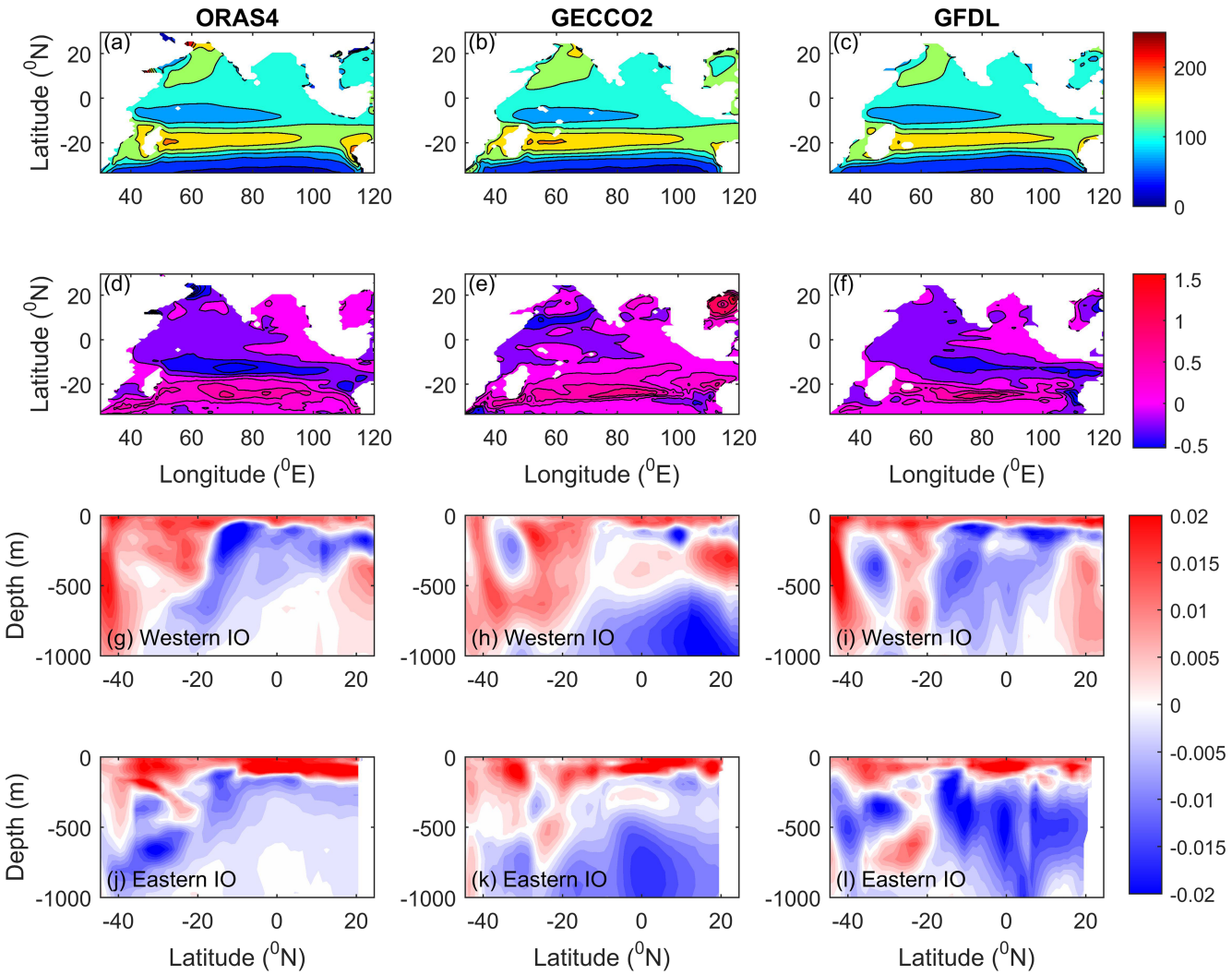

Figure 2. Mean thermocline depth (20°C isotherm) in the Indian Ocean (a, b, and c) and their respective trends in m/year (d, e, and f). Latitude-depth section of temperature trends in western (g, h, and i) and eastern (j, k, and l) Indian Ocean in degrees Celsius per year. ORAS4 = Ocean Reanalysis System 4; GECCO2 = German contribution to the consortium for Estimating the Circulation and Climate of the Ocean 2; GFDL = Ensemble Coupled Data Assimilation system by Geophysical Fluid Dynamics Laboratory; IO = Indian Ocean.

have attributed it to a 0.5° southward shift of the subtropical supergyre (Duan et al., 2013; Speich et al., 2007) in the IO with a consequent shift of IO mean thermal structure. This shift is induced by a global scale poleward shift in the westerly winds of the Southern Hemisphere (Jacobs, 2006; Thompson et al., 2000; Yang et al., 2007). Global scale oceanic response to the shift in subpolar westerly winds inferred from a model study also predicts warming around 40°S latitude (Oke & England, 2004) as inferred from the three reanalysis products. In GECCO2, as expected, consistent with the trends in thermocline depth, there is a subsurface weakening of cooling trends and warming in the western IO around 20°S. The observed cooling due to trends in local winds is found to be weakened. This could be due to the deepening of thermocline related to the decline in deep MOC. The results based on thermocline depth corroborate the theoretical aspects of Boccaletti (2004) and Boccaletti, Pacanowski, George, Philander, & Fedorov (2004), Boccaletti, Pacanowski, George, & Philander (2004) in this real-world scenario. The supergyre strength (horizontal stream function in the upper layers, $\gamma^n < 27.40$, averaged between 42°S and 32°S and 33°E and 50°E) and its position in the IO across the three products are also analyzed. ORAS4 and GFDL show an increasing trend (1961–2010) in the supergyre strength of 0.32 and 0.17 Sv/year, respectively. However,

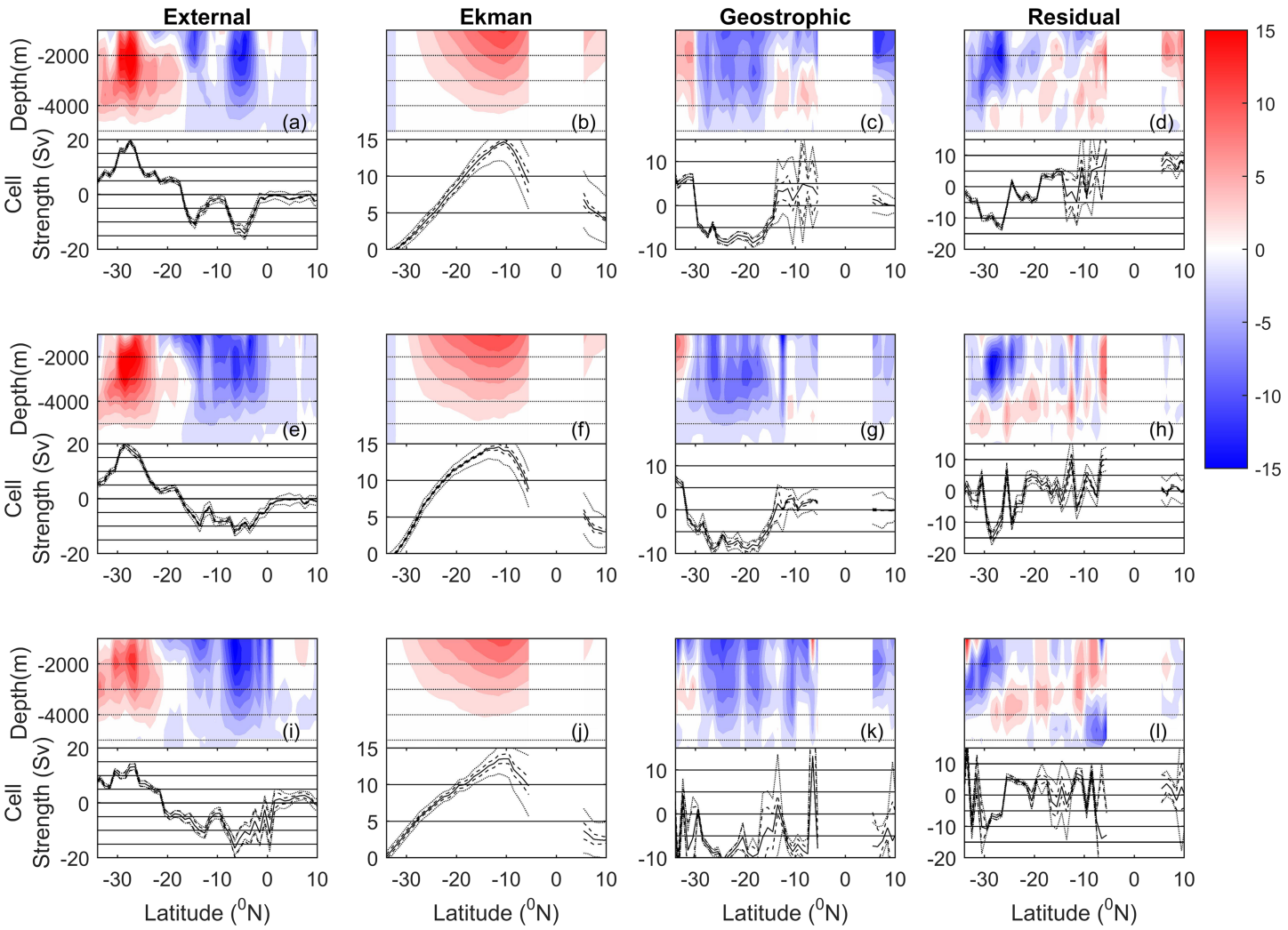

Figure 3. Various components of time mean meridional overturning circulation stream function in sverdrups (positive counterclockwise and negative clockwise) and their overturning cell strength in the Indian Ocean (1961–2010) in ORAS4 (a–d), GECCO2 (e–h), and GFDL (i–j). The thick lines show the mean, and the broken/thin lines show the interannual/seasonal standard deviation. ORAS4 = Ocean Reanalysis System 4; GECCO2 = German contribution to the consortium for Estimating the Circulation and Climate of the Ocean 2; GFDL = Ensemble Coupled Data Assimilation system by Geophysical Fluid Dynamics Laboratory.

GECCO2 shows only a weak trend of 0.03 Sv/year (not shown). Also, GECCO2 displays a negative trend during 1961–1985, while the other two display a weak positive trend. This is likely due to the decline of bottom layer transport in GECCO2, especially when the ITF transport is increasing in all three products albeit a relatively weak trend (not shown).

5. Decomposition of the IO Deep MOC

The decomposition of IO deep MOC into its three main components (external mode, geostrophic, and Ekman components) is presented (Figure 3). The three components and the residual which includes errors and ageostrophic components show similar characteristics across all three products. The residual components are found to be high mainly between 30°S and 20°S. This could be due to topographical influence as the local topography at these latitudes is highly varying. The external mode which is positive south of 20°S has a maximum of 20 Sv in ORAS4 and GECCO2, and 14 Sv in GFDL between 28°S and 26°S. A positive cell around 10°S can be noted in ORAS4 and GECCO2 (Figures 1a and 1b). Here, the maxima of the components consist of a strong negative contribution by the external mode (12–15 Sv) in all three products. However, both the Ekman component and geostrophic component are positive with a magnitude of 15 and 5 Sv,

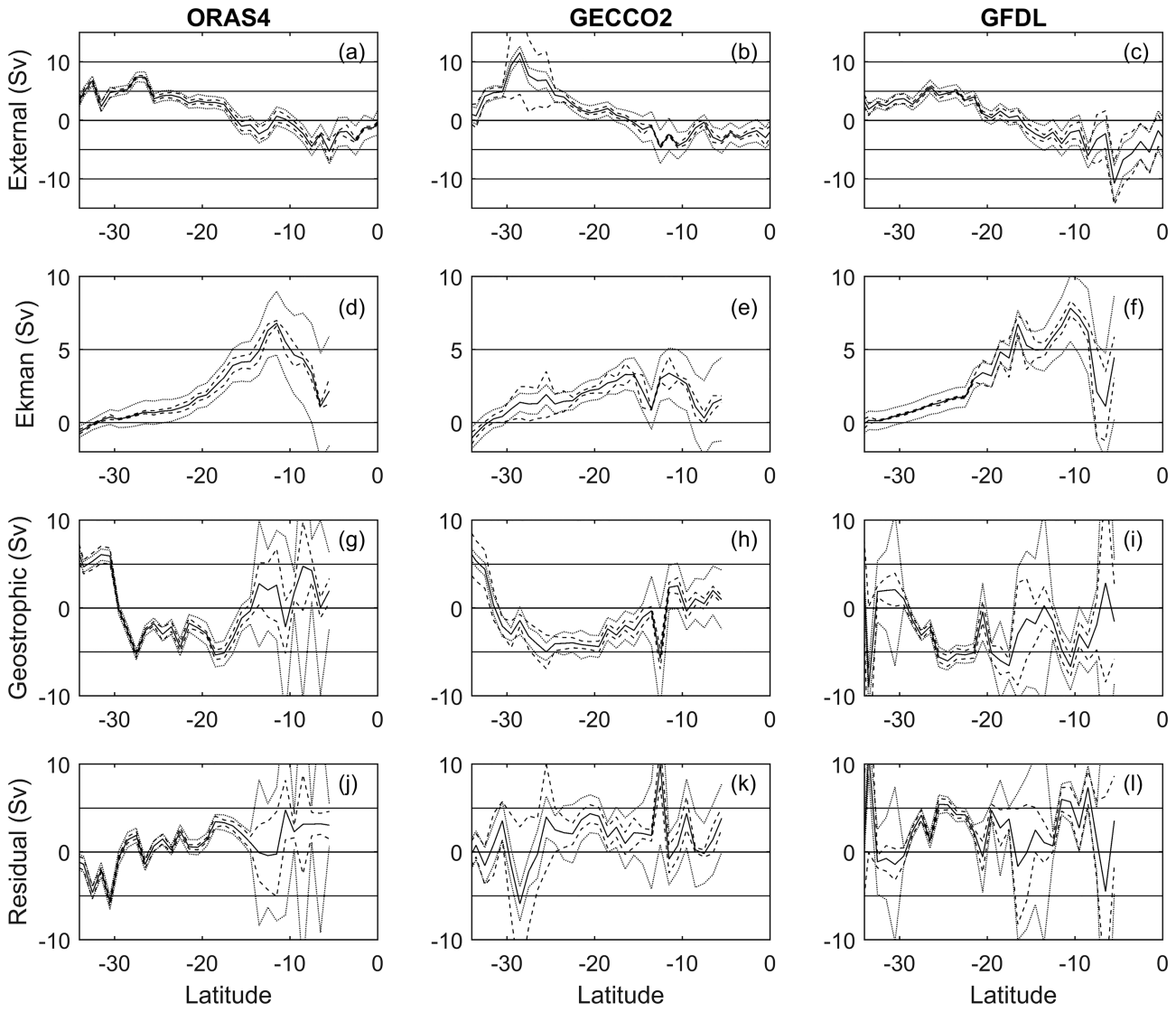

Figure 4. Various components of the time mean meridional overturning circulation stream function in sverdrups (positive counterclockwise and negative clockwise) in the Indian Ocean (1961–2010) in ORAS4 (a, d, g, and j), GECCO2 (b, e, h, and k), and GFDL (c, f, i, and l). The thick lines show the mean and the broken/thin lines show the interannual/seasonal standard deviation. ORAS4 = Ocean Reanalysis System 4; GECCO2 = German contribution to the consortium for Estimating the Circulation and Climate of the Ocean 2; GFDL = Ensemble Coupled Data Assimilation system by Geophysical Fluid Dynamics Laboratory.

respectively. It can be seen that in GFDL, at the same latitude, the total circulation is in the high negatives (Figure 1c). Here, the contribution by the geostrophic component is predominantly clockwise or negative. All together, the strong negative component around 10°S in GFDL is contributed by both the residual component of the MOC and geostrophic component. Here, no critical insights are drawn on the same from the decomposition of MOC other than that the differences in the vertical density structure result in different distribution of transports in GFDL compared to ORAS4 and GECCO2.

To gain further insights, the mean abyssal (depths below 4,000 m) velocity vectors in all the three products are investigated (Figure S6). The bathymetry in GFDL is found to be coarser in terms of resolution with thick walls between individual IO subbasins, while in the other two, the topographical barriers between basins are relatively thinner and discontinuous (especially the 90°E ridge which runs from 33°S to 17°N north along 90°E). The discrepancies in the bathymetry can at least partially explain the differences between GFDL and the other products at 10°S (Text S6). Clearly, these topographic differences also will result in differences in topographically generated waves, density structures, and

vertical and horizontal mixing which also contribute to the MOC. Unlike GFDL, both ORAS4 and GECCO2 are able to reproduce the IO abyssal circulation patterns as hindcasted by a high-resolution model (Srinivasan et al., 2009), but there is a steady decline of MOC in GECCO2. These combined with the validation of the products using sea level anomaly (Text S7) would lead us to conclude that ORAS4 is the most reliable among the three in terms of IO MOC.

We further analyze the contributions of each components to the MOC cell strength at the depths of observed maximum counterclockwise circulation (Figure 4). In ORAS4, the most reliable among the three, as per Figures 1a, 1d, and 1g, the maximum MOCs are south of 30°S (around 7 Sv at a depth of 2,000 m) and around 10°S (around 10 Sv at a depth of 3,000 m). GECCO2 would also display maximum MOCs at the same latitudes if its MOC did not decrease (Figures 1b and 1j–1l). The southern cell is found to be contributed by a combination of the external mode (Text S8) and geostrophic component (Figures 4a, 4b, 4g, and 4h). The cell at 10°S is found to be contributed by a combination of geostrophic and Ekman components (Figures 4d, 4e, 4g, and 4h). In summary, as per ORAS4 and GECCO2, it can be inferred that the geostrophic component is as significant as the Ekman component in the regional dynamics of the tropical IO MOC. Hence, both the slow deep circulation and rapid wind-driven circulation could be equally significant in determining the thermal structure and ocean heat uptake in the tropical IO.

6. Conclusions

The structure of the deep MOC in the IO in three ocean reanalysis products (ORAS4, GECCO2 and GFDL) is compared. All the three products are consistent with each other in simulating the dominant counterclockwise overturning cell located south of 30°S. This cell is dominated by the geopstrophic component and the external mode of the IO MOC. Another strong deep counterclockwise cell is evident at 10°S in ORAS4. At the same location, a weak counterclockwise cell is present in GECCO2, but a strong clockwise cell is seen in GFDL. The weak nature of the cell in GECCO2 is due to the steady decrease in the bottom meridional transport in GECCO2 unlike the other two. In GFDL, the clockwise cell is found to be the result of a low-resolution bathymetry where the 90°E ridge is too thick blocking the deep passages connecting west Australian basin and central Indian basin. Therefore, from the three reanalysis data sets studied, we infer that the IO Deep MOC is best represented in ORAS4. Based on ORAS4 and GECCO2, the inferred MOC consists of two deep and strong counterclockwise cells located south of 30°S and around 10°S. The cell at 10°S is due to the combination of Ekman and geostrophic components of the MOC. The role of mixing, horizontal and vertical resolutions, and surface forcing in generating these differences cannot easily be inferred, and such details are beyond the scope of the present study.

The slow deep circulation (MOC) along with the rapid shallow wind-driven circulation are the major components that determine the thermal structure as well as the ocean heat budget or the tropical heat uptake. Here, as per ORAS4 and GECCO2, both the geostrophic component and wind-driven circulation are found to be equally significant for tropical IO as they contribute significantly to the MOC. The response of the tropical IO thermocline to the decline in MOC is also investigated using GECCO2. In agreement with the model studies with hypothetical basins by Boccaletti, Pacanowski, George, Philander, & Fedorov (2004), Boccaletti, Pacanowski, George, and Philander (2004), the weakening of MOC in GECCO2 is found to be nullifying the cooling trends that prevail in the eastern tropical IO. In the western tropical IO, this cancelling effect is only partial, and it could be due to the strong influence of wind forcing in this region. Hence, it can be inferred that eastern tropical IO would be the first region to respond to any such long-term declining trends in MOC. Both ORAS4 and GFDL show an increasing trend in the IO subtropical supergyre strength, but there is only a weak trend in GECCO2. This could be due to the influence of the declining MOC on the supergyre. Comparative studies of reanalysis products (Jayasankar et al., 2019; Karmakar et al., 2018) in the IO with in situ and satellite observations finds ORAS4 to be the best with higher correlations and lower error. The results here also underscore the credibility of ORAS4 in the IO.

We could hardly overstate the importance of the low-frequency variability of the IO MOC and its role on the tropical IO response to anthropogenic forcing. Considering the tendency of the community to employ these reanalysis products as reality, this cautionary tale of the differences in them is very timely and important.

Acknowledgments

We acknowledge the financial support and computational resources provided by the Indian Institute of Technology, Bombay. The ocean reanalysis data sets (GECCO2, ORAS4, and GFDL) and respective wind data sets are downloaded from links provided by the University of Hamburg website (https://icdc.cen.uni-hamburg.de/daten.html). The ECMWF winds are downloaded from ECMWF website (http://apps.ecmwf.int/datasets/).

References

Alory, G., Wijffels, S., & Meyers, G. (2007). Observed temperature trends in the Indian Ocean over 1960–1999 and associated mechanisms. *Geophysical Research Letters*, *34*, L02606. https://doi.org/10.1029/2006GL028044

Balmaseda, M. A., Mogensen, K., & Weaver, A. T. (2013). Evaluation of the ECMWF ocean reanalysis system ORAS4. *Quarterly Journal of the Royal Meteorological Society*, *139*(674), 1132–1161. https://doi.org/10.1002/qj.2063

Balmaseda, M. A., Smith, G. C., Haines, K., Anderson, D., Palmer, T. N., & Vidard, A. (2007). Historical reconstruction of the Atlantic Meridional Overturning Circulation from the ECMWF operational ocean reanalysis. *Geophysical Research Letters*, *34*, L23515. https://doi.org/10.1029/2007GL031645

Boccaletti, G. (2004). Timescales and dynamics of the formation of a thermocline. *Dynamics of Atmospheres and Oceans*, *39*, 21–40.

Boccaletti, G., Pacanowski, R. C., George, S., & Philander, H. (2004). A diabatic mechanism for decadal variability in the tropics. *Dynamics of Atmospheres and Oceans*, *39*, 3–19.

Boccaletti, G., Pacanowski, R. C., George, S., Philander, H., & Fedorov, A. V. (2004). The thermal structure of the upper ocean. *Journal of Physical Oceanography*, *34*(4), 888–902. https://doi.org/10.1175/1520-0485(2004)034<0888:TTSOTU>2.0.CO;2

Dee, D. P., Uppala, S. M., Simmons, A. J., Berrisford, P., Poli, P., Kobayashi, S., et al. (2011). The ERA-Interim Reanalysis: Configuration and performance of the data assimilation system. *Quarterly Journal of the Royal Meteorological Society*, *137*(656), 553–597. https://doi.org/10.1002/qj.828

Du, Y., & Xie, S.-P. (2008). Role of atmospheric adjustments in the tropical Indian Ocean warming during the 20th century in climate models. *Geophysical Research Letters*, *35*, L08712. https://doi.org/10.1029/2008GL033631

Duan, Y., Hou, Y., Liu, H., & Liu, Y. (2013). The water mass variability and southward shift of the Southern Hemisphere mid-depth supergyre. *ActaOceanologica Sinica*, *32*(11), 74–81. https://doi.org/10.1007/s13131-013-0380-7

Fujii, Y., Tsujino, H., Toyoda, T., & Nakano, H. (2017). Enhancement of the southward return flow of the Atlantic Meridional Overturning Circulation by data assimilation and its influence in an assimilative ocean simulation forced by CORE-II atmospheric forcing. *Climate Dynamics*, *49*(3), 869–889. https://doi.org/10.1007/s00382-015-2780-1

Ganachaud, A., & Wunsch, C. (2000). Improved estimates of global ocean circulation, heat transport and mixing from hydrographic data. *Nature*, *408*(6811), 453–457. https://doi.org/10.1038/35044048

Ganachaud, A., Wunsch, C., Marotzke, J., & Toole, J. (2000). Meridional overturning and large-scale circulation of the Indian Ocean. *Journal of Geophysical Research*, *105*(C11), 26,117–26,134. https://doi.org/10.1029/2000JC900122

Guemas, V., Corti, S., Garcia-Serrano, J., Doblas-Reyes, F. J., Balmaseda, M., & Magnusson, L. (2013). The Indian Ocean: The region of highest skill worldwide in decadal climate prediction. *Journal of Climate*, *26*(3), 726–739. https://doi.org/10.1175/JCLI-D-12-00049.1

Han, W., Meehl, G. A., & Hu, A. (2006). Interpretation of tropical thermocline cooling in the Indian and Pacific Oceans during recent decades. *Geophysical Research Letters*, *33*, L23615. https://doi.org/10.1029/2006GL027982

Han, W., Meehl, G. A., Rajagopalan, B., Fasullo, J. T., Hu, A., Lin, J., et al. (2010). Patterns of Indian Ocean sea-level change in a warming climate. *Nature Geoscience*, *3*(8), 546–550. https://doi.org/10.1038/ngeo901

Hermes, J. C., & Reason, C. J. (2008). Annual cycle of the south Indian Ocean (Seychelles-Chagos) thermocline ridge in a regional ocean model. *Journal of Geophysical Research*, *113*, C04035. https://doi.org/10.1029/2007JC004363

Jacobs, S. (2006). Observations of change in the Southern Ocean. *Philosophical Transactions of the Royal Society A: Mathematical, Physical and Engineering Sciences*, *364*(1844), 1657–1681. https://doi.org/10.1098/rsta.2006.1794

Jayasankar, T., Eldho, T. I., Ghosh, S., & Murtugudde, R. (2019). Assessment of the interannual variability of local atmospheric and ITF contribution to the subsurface heat content of southern tropical Indian Ocean in GECCO2 and ORAS4 using ROMS. *Global and Planetary Change*, *181*, 102974. https://doi.org/10.1016/j.gloplacha.2019.05.014

Jin, X., Kwon, Y.-O., Ummenhofer, C. C., Seo, H., Kosaka, Y., & Wright, J. S. (2018). Distinct mechanisms of decadal subsurface heat content variations in the eastern and western Indian Ocean modulated by tropical Pacific SST. *Journal of Climate*, *31*(19), 7751–7769. https://doi.org/10.1175/JCLI-D-18-0184.1

Kalnay, E., Kanamitsu, M., Kistler, R., Collins, W., Deaven, D., Gandin, L., et al. (1996). The NCEP/NCAR 40-year reanalysis project. *Bulletin of the American Meteorological Society*, *77*(3), 437–471. https://doi.org/10.1175/1520-0477(1996)077<0437:TNYRP>2.0.CO;2

Karmakar, A., Parekh, A., Chowdary, J. S., & Gnanaseelan, C. (2018). Intercomparison of tropical Indian Ocean features in different ocean reanalysis products. *Climate Dynamics*, *51*(1-2), 119–141. https://doi.org/10.1007/s00382-017-3910-8

Karspeck, A. R., Stammer, D., Köhl, A., Danabasoglu, G., Balmaseda, M., Smith, D. M., et al. (2017). Comparison of the Atlantic Meridional Overturning Circulation between 1960 and 2007 in six ocean reanalysis products. *Climate Dynamics*, *49*(3), 957–982. https://doi.org/10.1007/s00382-015-2787-7

Köhl, A. (2015). Evaluation of the GECCO2 ocean synthesis: Transports of volume, heat and freshwater in the Atlantic. *Quarterly Journal of the Royal Meteorological Society*, *141*(686), 166–181. https://doi.org/10.1002/qj.2347

Lee, T., & Marotzke, J. (1998). Seasonal cycles of meridional overturning and heat transport of the Indian Ocean. *Journal of Physical Oceanography*, *28*(5), 923–943. https://doi.org/10.1175/1520-0485(1998)028<0923:SCOMOA>2.0.CO;2

Levitus, S., Antonov, J., & Boyer, T. (2005). Warming of the world ocean, 1955–2003. *Geophysical Research Letters*, *32*, L020604. https://doi.org/10.1029/2004GL021592

Luyten, J. R., Pedlosky, J., & Stommel, H. (1983). The ventilated thermocline. *Journal of Physical Oceanography*, *13*(2), 292–309. https://doi.org/10.1175/1520-0485(1983)013<0292:TVT>2.0.CO;2

Murtugudde, R., & Annamalai, H. (2004). Role of the Indian Ocean in regional climate variability. *Geophysical Monograph*, *147*, 213–246. https://doi.org/10.1029/147GM13

Murtugudde, R., & Busalacchi, A. J. (1999). Interannual variability of the dynamics and thermodynamics of the tropical Indian Ocean. *Journal of Climate*, *12*(8), 2300–2326. https://doi.org/10.1175/1520-0442(1999)012<2300:IVOTDA>2.0.CO;2

Murtugudde, R., Busalacchi, A. J., & Beauchamp, J. (1998). Seasonal-to-interannual effects of the Indonesian throughflow on the tropical Indo-Pacific Basin. *Journal of Geophysical Research*, *103*(C10), 21,425–21,441. https://doi.org/10.1029/98JC02063

Oke, P. R., & England, M. H. (2004). Oceanic response to changes in the latitude of the Southern Hemisphere subpolar westerly winds. *Journal of Climate*, *17*(5), 1040–1054. https://doi.org/10.1175/1520-0442(2004)017<1040:ORTCIT>2.0.CO;2

Pillai, P. A., & Mohankumar, K. (2009). Role of TBO and ENSO scale ocean-atmosphere interaction in the Indo-Pacific region on Asian summer monsoon variability. *Theoretical and Applied Climatology*, *97*(1-2), 99–108. https://doi.org/10.1007/s00704-008-0053-1

Schwarzkopf, F. U., & Böning, C. W. (2011). Contribution of Pacific wind stress to multi-decadal variations in upper-ocean heat content and sea level in the tropical south Indian Ocean. *Geophysical Research Letters*, *38*, L12602. https://doi.org/10.1029/2011GL047651

Sen, P. K. (1968). Estimates of the regression coefficient based on Kendall's tau. *Journal of the American Statistical Association*, *63*(324), 1379–1389. https://doi.org/10.1080/01621459.1968.10480934

Sime, L. C., Stevens, D. P., Heywood, K. J., & Oliver, K. I. (2006). A decomposition of the Atlantic meridional overturning. *Journal of Physical Oceanography*, *36*(12), 2253–2270. https://doi.org/10.1175/JPO2974.1

Speich, S., Blanke, B., & Cai, W. (2007). Atlantic Meridional Overturning Circulation and the Southern Hemisphere supergyre. *Geophysical Research Letters*, *34*, L23614. https://doi.org/10.1029/2007GL031583

Srinivasan, A., Garraffo, Z., & Iskandarani, M. (2009). Abyssal circulation in the Indian Ocean from a 1/12° resolution global hindcast. *Deep Sea Research Part I: Oceanographic Research Papers*, *56*(11), 1907–1926. https://doi.org/10.1016/j.dsr.2009.07.001

Theil, H. (1950). A rank-invariant method of linear and polynomial regression analysis, I, II, III. *Nederlandse Akademie Wetenschappen, Proceedings*, *53*, 386–392. 521--525, 1397--1412

Thompson, D. W., Wallace, J. M., & Hegerl, G. C. (2000). Annular modes in the extratropical circulation. Part II: Trends. *Journal of Cimate*, *13*, 1018–1036. https://doi.org/10.1175/1520-0442(2000)013<1000:AMITEC>2.0.CO;2

Ummenhofer, C. C., Biastoch, A., & Böning, C. W. (2017). Multidecadal Indian Ocean variability linked to the Pacific and implications for preconditioning Indian Ocean dipole events. *Journal of Climate*, *30*(5), 1739–1751. https://doi.org/10.1175/JCLI-D-16-0200.1

Uppala, S. M., Kållberg, P. W., Simmons, A. J., Andrae, U., Bechtold, V. D., Fiorino, M., et al. (2005). The ERA-40 Re-analysis. *Quarterly Journal of the Royal Meteorological Society*, *131*(612), 2961–3012. https://doi.org/10.1256/qj.04.176

Valsala, V., Maksyutov, S., & Murtugudde, R. (2010). Possible interannual to interdecadal variabilities of the Indonesian throughflow water pathways in the Indian Ocean. *Journal of Geophysical Research*, *41*, 1921. https://doi.org/10.1175/2011JPO4561.1

Wang, W., Köhl, A., & Stammer, D. (2012). The deep meridional overturning circulation in the Indian Ocean inferred from the GECCO synthesis. *Dynamics of Atmospheres and Oceans*, *58*, 44–61. https://doi.org/10.1016/j.dynatmoce.2012.08.001

Wang, W., Zhu, X., Wang, C., & Köhl, A. (2014). Deep meridional overturning circulation in the Indian Ocean and its relation to Indian Ocean Dipole. *Journal of Climate*, *27*(12), 4508–4520. https://doi.org/10.1175/JCLI-D-13-00472.1

Yang, X.-Y., Huang, R. X., & Wang, D. X. (2007). Decadal changes of wind stress over the Southern Ocean associated with Antarctic ozone depletion. *Journal of Climate*, *20*(14), 3395–3410. https://doi.org/10.1175/JCLI4195.1

Zhang, S., Harrison, M. J., Rosati, A., & Wittenberg, A. (2007). System design and evaluation of coupled ensemble data assimilation for global oceanic climate studies. *Monthly Weather Review*, *135*(10), 3541–3564. https://doi.org/10.1175/MWR3466.1

Zhuang, W., Feng, M., Du, Y., Schiller, A., & Wang, D. (2013). Low-frequency sea level variability in the southern Indian Ocean and its impacts on the oceanic meridional transports. *Journal of Geophysical Research: Oceans*, *118*, 1302–1315. https://doi.org/10.1002/jgrc.20129